Machine Learning-Based Integrated Wireless Sensing and Positioning for Cellular Network

Lei Zhang, *Member, IEEE*, Xin Chu, and Menglin Zhai, *Member, IEEE*

***Abstract*— Integrated sensing and communication (ISAC) is one of the most promising technical directions in B5G/6G era. Nevertheless, it is challenging for network operators to provide proper human-centric services (HCSs), appropriately with the explosive growth of mobile terminals in constantly changing scenarios. Scenario sensing is the foundation to provide users with intelligent context-aware services, while the combination of machine learning (ML) and automatic data collection enables network operators to become more flexible in decision-making and planning. In this article, an ML-based integrated indoor/outdoor (IO) sensing and positioning framework is proposed to improve the potential of ML in the context of cellular network service management. First, large amounts of measurement reports (MRs) are collected over Layer 3 at user equipment (UE) and evolved NodeBs (eNBs) in urban areas, including both indoor and outdoor samples to simulate the minimization of drive test (MDT). Then, a random-forest-based IO classifier is implemented to sense the mobile scenarios and filter the positioning fingerprints. Subsequently, the weighted *K*-nearest neighbor (WKNN)-based Enhanced Cell ID (ECID) merging with the MR method is used for cellular positioning. The performance evaluation has shown that the positioning error of the MRs after denoising is effectively reduced compared with the conventional fingerprint-based positioning. Specifically, under the 67% standard defined by Federal Communications Commission (FCC), the resulting positioning error is about 4% lower than the case without preprocessing. In addition, comparative experiments are conducted to discuss the impact of different *K* values at different data sizes of fingerprints. Moreover, the further data analysis shows that MRs collected in the mild indoor (MI) scenarios have a positive effect on the overall positioning error, which indicates that refined contextualizations contribute to the cellular positioning for HCS upgrade.**

***Index Terms*— Cellular network, human-centric service (HCS), integrated sensing and communication (ISAC), machine learning (ML), radio frequency (RF) fingerprinting positioning.**

I. Introduction

HUMAN-centric service (HCS)-based applications have been greatly boosted by the rapid development and spread of the Internet-of-Things (IoT) and intelligent terminals over the past decade. The next-generation mobile communication system (B5G/6G) is expected to build an integrated sensing and communication (ISAC) framework enabled by 5G ultradense cellular networks [1]. In this case, the cellular system is used as a large-scale network sensor to measure the surrounding environment based on wireless perception and provide environment and location awareness services in a spectrum/energy/cost-efficient way [2]. On one hand, 6G research has been reviewed by higher frequency bands, wider bandwidths, and larger antenna arrays to provide better personalized service [3], [4]; On the other hand, machine learning (ML) has been used to improve user service systems and address new challenges [5], such as ML-based indoor/outdoor (IO) detection that is proposed to adjust the network to enhance the environment type-based user services.

The global navigation satellite system (GNSS)-based positioning method basically satisfies the criteria of outdoor positioning, yet it is limited in the confined environments, such as urban canyon and overpass. This is due to the shielding effect on satellite signals, which results in satellite researching in a time-consuming way. To shorten the time delay, radio frequency (RF) fingerprinting positioning has been integrated into long-term evolution (LTE) architecture by 3GPP to provide outdoor emergency positioning services, such as enhanced 911 (E911) [6], [7], [8], [9]. RF fingerprinting positioning provides complementary or alternative GPS-related information by comparing the similarity between the user's received signal strength and this fingerprint database [10], [11]. Currently, RF fingerprinting positioning is widely adopted in various networks, which can be extended as endogenetic sensor, without major replacements to the network infrastructure [12], [13].

At present, wireless network testing has shifted to user active reporting mode to replace the traditional drive test with consuming large amounts of the manpower and material resources, large capital investment, and long test cycle. 3GPP release 10 (TR 32.827) opens the opportunity to collect data autonomously from mobile devices, which is also called minimization of drive test (MDT). The cellular big data including RF fingerprints collected in the MDT method are cost-effective for operators and carbon-neutral for the public [14]. However, since the data collected by MDT through the terminals are automatically reported by users, the indoor and outdoor measurement reports (MRs) are jumbled up in the database, which is able to affect the positioning performance. In some cases, mobile devices entering the room from outside still retain outdoor GPS information, so these

Manuscript received 20 August 2022; revised 4 November 2022; accepted 11 November 2022. Date of publication 24 November 2022; date of current version 18 January 2023. This work was supported in part by the National Natural Science Foundation of China (NSFC) under Grant 61901104 and Grant 61801107 and in part by the Science and Technology Research Project of Shanghai Songjiang District under Grant 20SJKJGG4C. The Associate Editor coordinating the review process was Dr. Valentina Bianchi. *(Corresponding author: Menglin Zhai.)*

The authors are with the College of Information Science and Technology, Donghua University, Shanghai 201620, China (e-mail: lei.zhang@dhu.edu.cn; 2201795@mail.dhu.edu.cn; mlzhai@dhu.edu.cn).

Digital Object Identifier 10.1109/TIM.2022.3224513

TABLE I
COMPARISON OF SOLUTIONS FOR IO CLASSIFICATION

Ref.	Data	Method	Accuracy
[15]	GPS, Temperature	Time-activity Diary	81-91%
[16]	GPS, Signal strength	Decision Tree	89-98%
[17]	GPS, Signal strength	Hidden Markov Model	92-99%
[18]	iBeacons	BlueDetect	96%
[20]	Magnetometer	Naive Bayes	83%
[21]	Cell data, Light Sensor	State Machine	98%
[22]	Cell data, Light Sensor, and Magnetometer	IODetector	92%
[24]	Cell data	KNN	97%

kind of indoor data carry drifted GPS information, as well as the indoor devices near windows or exits. These data samples collected as fingerprints cannot represent the real position of the devices, which can be regarded as noise for positioning. Due to the poor regularity of pedestrian movement and limited actual measured data, the recognition of indoor and outdoor scenarios using communication data is of importance for contextualizing network operations including positioning error reduction.

Perception and classification of IO scenarios is the prerequisite of interference elimination. The most common method is to rely on GNSS signals that cannot cover indoors to form positioning for judgment. Nevertheless, regardless of the time delay or the possible deviation of GPS in a semi-indoor scenario, it is unreliable to solely rely on GPS for IO classification. Lee et al. [15] use GPS and temperature data to classify IO, and the accuracy is about 85%. Table I shows the comparison of various solutions for IO classification. Pissardini and Fonseca Junior [16] construct a decision tree using different parameters including signal strength for IO classification. The highest accuracy evaluated on the real datasets reaches to 98%. Zhu et al. [17] exploit a hidden Markov model with stacking ensemble, which achieves an accuracy up to 99%. Zou et al. [18] make use of iBeacons for IO classification, and Mizuno et al. [19] use beacons and GPS information for indoor and outdoor scenarios, respectively, but the limitations including sensor installation and operator cost make these solutions difficult to be applied on a large scale. Ashraf et al. [20] use the magnetometer widely present in mobile phones to separate IO samples and the achieved accuracy based on naive Bayes is 83%. Liu et al. [21] harness the cellular data collected by the smart phone merging with the light sensor to classify IO scenarios and the resulting accuracy is above 98%. Li et al. [22] build a radio map using the light intensity and magnetism in combination with the cellular data and achieve the classification accuracy up to 92%. Li et al. [23] use light intensity and WiFi signal for the weak learner to detect "indoor, outdoor, and semi-open" (IOS). Wang et al. [24] divide the IO classification into four different labels and calculate the statistical features to train a classifier. The K-nearest neighbor (KNN)-based method reaches an accuracy up to 97%. In addition, Rodriguez et al. [25] and Kaya and Calin [26] discuss the scheme of classification based on the differences between IO scenarios in terms of radio propagation.

The advantages and disadvantages of different localization models and architectures are shown in Table II. Recent 3GPP NR positioning systems support solutions of observed time difference of arrival (OTDOA) [27], uplink time difference of arrival (UTDOA), angle information, multicell round trip time (Multi-RTT), and Enhanced Cell ID (ECID) in Release 16 [28], [29]. In the LTE system, the ECID method is widely used for positioning based on the received signal strength, which exploits radio measurements to determine a distance to the terminal. Therefore, this method can also be treated as a fingerprinting method [30]. Aly and Youssef [31] match the cellular fingerprints with the information collected by the built-in sensor of the mobile phone to further improve the performance of the entire positioning system. Tian et al. [32] propose to exploit the subspace identification approach for large-scale RF fingerprints' prediction and it is proven effectively that it improves the positioning performance in urban outdoor scenes. Viel et al. [33] propose a new map-matching algorithm that exploits the hidden Markov model and random forests to process noisy and sparse cellular signal. In [34], the performance of random-forest-based fingerprinting positioning is further improved by considering problems related to signal variations in communication issues, multipath fading, and surrounding interference. ML has been studied to improve the performance of positioning system [35], [36]. Butt et al. [37] minimize the position error of the mobile users by building feature vectors based on deep learning. Prasad et al. [38] propose a supervised ML approach based on Gaussian process regression to position users in a distributed massive multiple-input–multiple-output system (DM-MIMO). Sou et al. [39] exploit a particle Markov chain model for indoor localization on wireless fingerprint systems. Polak et al. [13] provide an extensive performance study of different ML algorithms to improve RF fingerprinting-based indoor localization.

To our best knowledge, there is no integrated research on IO sensing and positioning based on RF communication signals for cellular network operation. This article presents an experimental study for IO sensing-assisted RF fingerprinting positioning. Our main contributions are as following.

1) More than 56 000 MRs are collected in a real urban area covered by the commercial cellular network. The test scenarios include most of the main roads and seven different indoor scenarios in this area.
2) An ML-based integrated IO sensing and positioning framework is proposed to sense the mobile scenarios and reduce the RF fingerprinting positioning error. The positioning results show that denoising the database by IO classifier can effectively reduce the RF fingerprinting positioning error up to 4% under Federal Communications Commission (FCC) positioning standard.
3) The positioning performance is evaluated by different data sizes and parameters of the positioning algorithm. The further data analysis shows that the setting of these parameters has an impact on the positioning error, and the MRs collected in the mild indoor (MI) scenarios have a positive effect on the overall positioning error. In this case, further classification for database is carried out on

TABLE II
SUMMARY OF DIFFERENT LOCALIZATION ARCHITECTURES AND TECHNOLOGIES

Model	**Technology**	**Advantage**	**Disadvantage**
Geometric-based	Time of Arrival (TOA)	High accuracy	Time sync is required; LoS propagation is assumed
	Time Difference of Arrival (TDOA)	High accuracy; Time sync is dispensable	LoS propagation is assumed
	Angles of Arrival (AOA)	Time sync is dispensable; Only two anchor nodes (ANs) are needed	Low accuracy in dense urban; Directional beams are required
	Received Signal Strength (RSS)	Time sync is dispensable; LoS is not mandatory	Low accuracy; Vulnerable in complex environments
Scene analysis-based	Fingerprints	Very high accuracy; Robust to clutter environments; LoS is not mandatory	Fingerprint database is indispensable in offline phase
Proximity-based	RSS/Cell-ID (CID)	Simple and inexpensive; Easy to implement; Short response time	Low accuracy; Rely on the density of base stations
Localization architecture	**Example**	**Advantage**	**Disadvantage**
GNSS-based	GPS	High accuracy; Global positioning; Interface is free to call at anytime	Power consumption; Vulnerable to weather and complex environments; Indoor positioning is not possible
Cellular network-based	2G: CID+TA/E-OTD 3G: CID+RTT/OTDOA/A-GPS 4G: ECID/OTDOA/UTDOA/ A-GNSS 5G: ECID/UTDOA/DTDOA/ UAOA/Multi-RTT	High success rate; Flexibility and Mobility; Unaffected by weather and location	Lower accuracy; The terminal can not be actively positioned
Wi-Fi-based	IEEE 802.11	High accuracy and speed; Flexibility and Mobility; Easy to install	Must be online; Intensive deployment is required
UWB-based	IEEE 802.15.4a	High accuracy; Low power consumption; Strong anti-interference ability	High cost; Low spectrum utilization

the basis of IO classification to refine this framework of integrated IO sensing and positioning.

The rest of this article is organized as follows. Section II describes the actual measurement campaign and presents the information contained in the MRs. Section III describes the ML-based integrated IO sensing and positioning framework. Section IV shows the experimental results, discusses the effects of different parameters on localization, and refines scene classification. Finally, we conclude our work in Section V.

II. MEASUREMENT CAMPAIGN

In the MDT system, the users upload MRs automatically, so the mobile terminals are able to use the run-time database to locate. For complying with the trend of MDT continuously replacing the traditional drive test, the measurement data are collected by *TEMS INVESTIGATION* [40] from a realistic urban area in China, which is covered by the commercial cellular network. We simulate the process of collecting MRs automatically in the MDT system through the actual drive test with intensive sampling, which has practical significance for further HCS.

The specific measurement configuration in the LTE network is shown in Table III. At each sampling point, the information from a serving cell and several neighboring cells is able to be monitored. During the actual drive test of simulating MDT, the continuous data service is applied to collect MRs by the fixed test device on a driving car (see Fig. 1) and record the raw data MRs for postprocessing.

TABLE III
CELLULAR CONFIGURATIONS AND MEASUREMENT PLATFORM

Item	**Description**
Network protocol	FDD-LTE
Frequency	1.85 GHz
Reference Signal Transmit Power	40/ 80 dBm
Serving cell	≤ 1
Neighboring cells	≤ 6
Test device	Samsung S5 G900I
Data acquisition	TEMS App v16

A variety of information are contained in MRs,[1] including the cell ID and the corresponding reference signal received power (RSRP) of the serving cell and its six neighboring cells. The staple network key indicators are described as follows.

1) *E-UTRAN Cell Identifier:* The unique identifier of the cell.
2) *Latitude & Longitude:* The recorded GPS coordinates of the user equipment (UE).

[1]The dataset and code are available at https://github.com/Code-Dataset/Integrated-Sensing-And-Positioning.

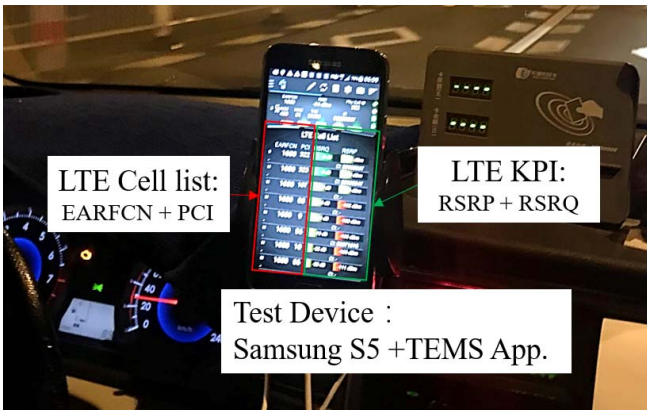

Fig. 1. Schematic of the measurement campaign.

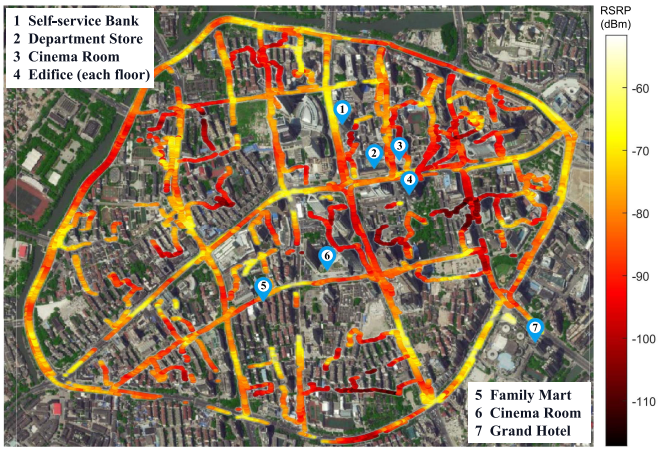

Fig. 2. Measurement sites and RSRP distributions.

3) *RSRP & Reference Signal Received Quality (RSRQ):* Indicators of received signal strength and quality, as the main metrics for IO classification and RF fingerprinting positioning.
4) *Timing Advance (TA):* Transmission timing between the UE and the eNodeB.

During the moving process of UE, the KPIs of MRs vary among scenarios and locations due to the coverage of different evolved NodeBs (eNBs). For example, Fig. 2 shows the change in RSRP of the outdoor data samples. Therefore, the fingerprint-based scenario sensing is performed to further investigate the positioning error change. Specifically, the outdoor measurement is carried out in different ways on the main roads and some branches, and the indoor data samples are collected in various indoor scenarios. Seven specific test points are indicated in Fig. 2 to show the diversity of indoor scenarios. GPS signal is unable to be detected in the deep indoor (DI) scenarios like the shopping mall, which results in unsuccessful positioning. Our measurement campaign approves the MI scenarios, where the indoor samples collected close to the windows have deviations from the actual GPS coordinates. Therefore, it is necessary to classify the scenarios and denoise the data before localization, which is beneficial to improve the positioning accuracy for a specific scene.

III. Scheme Design

Since the positioning error is affected by the deviation of the indoor MRs, the scheme is devised to reduce the positioning error by filtering the positioning fingerprints through ML before positioning. This design is mainly divided into two parts. A random-forest-based IO classifier is implemented to sense the mobile scenarios and preprocess the database for filtering the positioning fingerprints in the first part. In the second part, the weighted K-nearest neighbor (WKNN)-based ECID method is used for RF fingerprinting positioning. Subsequently, we compare and evaluate the system performance quantitatively from different aspects.

The scheme process is shown in Fig. 3. "I + O" means that there are both indoor and outdoor fingerprints in the database before IO classification, and "O" means that only outdoor fingerprints are contained in the database after denoising.

A. Random-Forest-Based IO Classification

Ensemble learning accomplishes the learning tasks by constructing and combining multiple base learners, which aims at predicting the target value (scenario label) of the test set based on the original measured data effectively. Compared with a single decision tree, a random forest gathers the predictions of all individual trees in the training process, and the final prediction is made based on the majority of votes which can lead to better classification results.

Feature engineering refers to the process of converting the initial data into the model training data, and then obtaining better training data features to improve the model performance, which mainly includes feature extraction and feature selection. The MRs are divided into the training set and test set. We build the KPI-based feature engineering combined with the characteristics of radio propagation to train random forest and label samples for indoor and outdoor. Then the trained model is adopted to classify the test set.

The previous work in [41] demonstrates that random-forest-based IO classification is more suitable for processing cellular big data with multiple features and 20 variables can be used to classify effectively. For example, the RSRP and RSRQ of hearable cell are directly used to determine indoor and outdoor scenarios; UEs located at the edge of the cell can be judged by calculating the difference between the RSRP and RSRQ of the serving cell and the strongest neighboring cell; the difference between the RSRP estimated through the Cost 231 Hata channel model and the measured RSRP of the serving cell is calculated as the IO classification feature, and the formula is as follows:

$$\Delta\text{RSRP} = \text{RSTP} - (46.3 + 33.9\log(f) + 44.9\log(78T_a) + C) - \text{RSRP} \quad (1)$$

where f and C denote the carrier frequency and correct factor (=3 for metropolitan areas), respectively. T_a represents the TA.

There are about 29% of the samples which are excluded from the bootstrap sample during the algorithm operation, which are called the out-of-bag (OOB) data. Fig. 4 shows that the OOB error is lower than 3% and converges when reaching 20 growing trees. Since the OOB error and the accuracy of

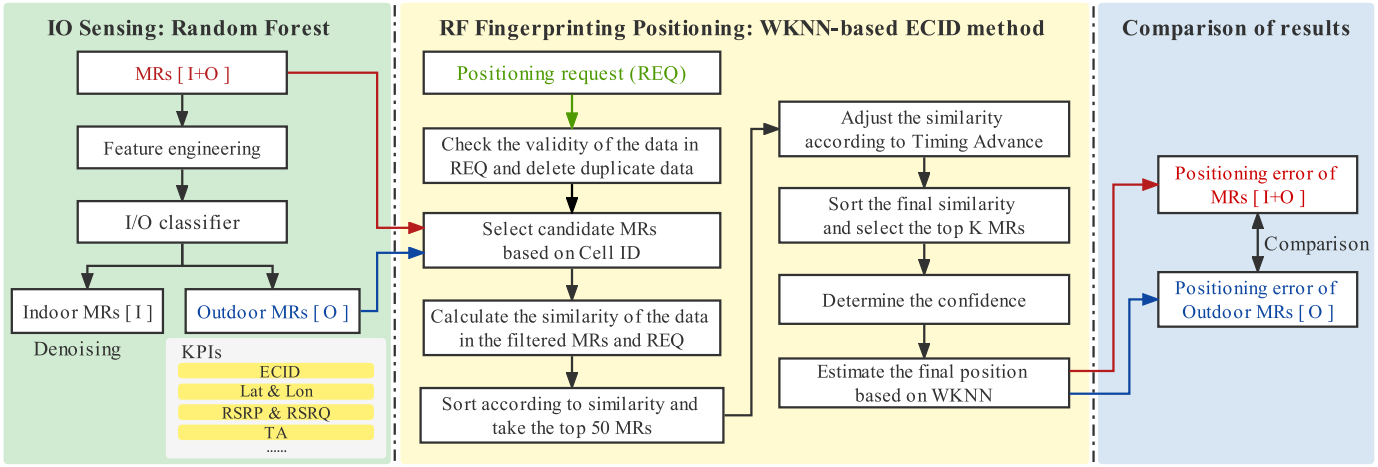

Fig. 3. Scheme flowchart.

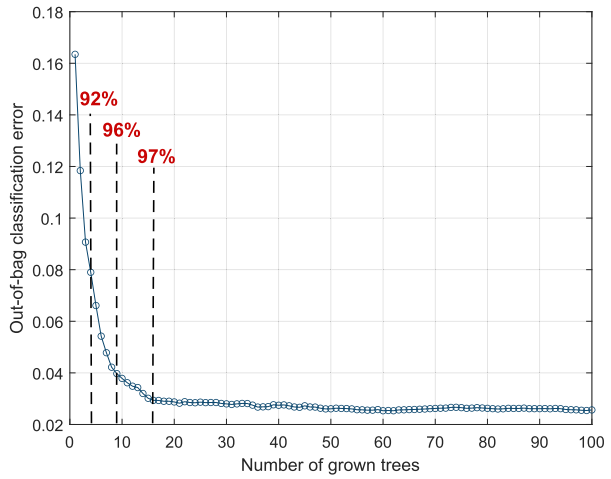

Fig. 4. OOB error with the growing of decision trees in random-forest-enabled IO classification.

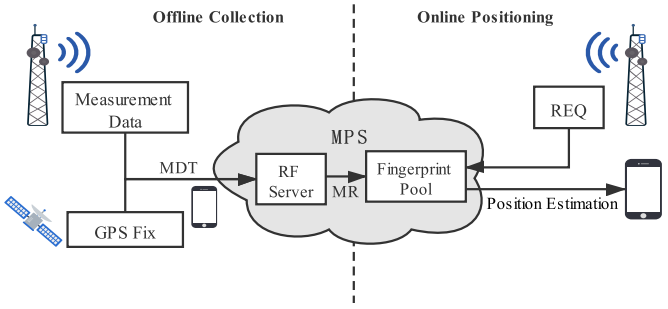

Fig. 5. RF fingerprinting positioning schematic.

the ensemble model are complementary, which further shows that the classification accuracy of this model reaches 97%.

Accurate IO classification result is beneficial to remove the interference of indoor fingerprints, which is the basis for improving the positioning accuracy. After classifying the IO scenarios effectively, we remove the indoor MRs that deviate from the actual location based on their labels. Subsequently, the raw MRs containing both the outdoor and indoor fingerprints and the denoised outdoor MRs are used as databases for positioning to discuss the impact of the ML-based fingerprint denoising on the positioning performance.

B. Improved WKNN-Based RF Fingerprinting Positioning

The RF fingerprint-based positioning method mainly includes two stages: offline collection and online positioning, as shown in Fig. 5. During the offline collection process, large amounts of radio measurements in different scenarios are collected by the mobile device through the simulated MDT and imported into the mobile positioning system (MPS). The RF server compresses the radio measurements into a size-efficient data file for the serving mobile positioning center to use. The MR-based fingerprint database is stored by MPS, which provides high-precision positioning service. In the online positioning step, the real-time positioning request (REQ) reported by UE is compared with all the historical samples stored in the database. Ultimately, the MPS calculates the correlation between them to estimate the current position.

The WKNN-based ECID merging with MR method is used for cellular positioning, and the specific steps of the algorithm are demonstrated in Fig. 3. First, checking the validity of the data in the positioning REQ and deleting duplicate data. Using the data filtering mechanism, the fingerprints far away from the user are filtered from the fingerprint database according to the number of neighboring cells. Then, calculating the similarity based on RSRP by least mean square (LMS) to take the top 50 fingerprint records, and adjusting the similarity according to TA to take the top K fingerprints. Finally, determining the confidence and using the similarity as the weight coefficient in the WKNN algorithm to calculate the final position, which is represented by the latitude and longitude of the center of the generated ellipse.

1) Data Filtering Mechanism and Similarity Calculation: Due to thousands of fingerprint records in the fingerprint database, the positioning speed and accuracy are greatly affected without a suitable data filtering mechanism. Therefore, the main purpose of data screening is to perform matching calculations within a limited area according to the number of neighboring cells and find candidate MRs in the fingerprint database to reduce the positioning error and the amount of calculation. Specifically, when the REQ has one neighboring

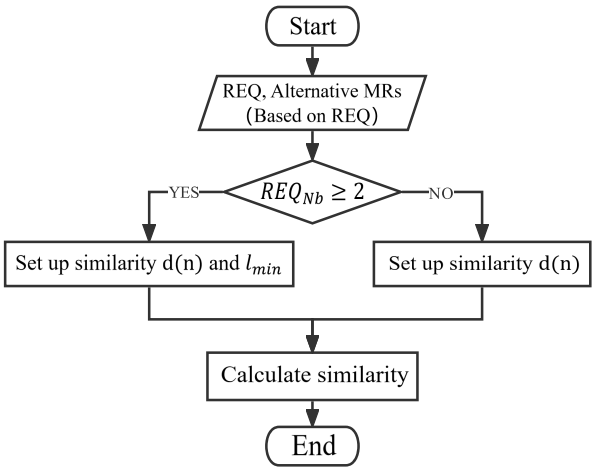

Fig. 6. Similarity calculation flowchart.

cell ($\mathrm{REQ_{Nb}} = 1$), we first try to find the MRs with only one neighboring cell in the fingerprint database ($\mathrm{MR_{Nb}} = 1$), and then it is strictly required that the serving cell ID ($\mathrm{Serv_{ID}}$) and the first neighboring cell ID ($\mathrm{Nb1_{ID}}$) of the selected MR and REQ are the same, respectively. If no such MR is found, the condition that the RSRP of the second neighboring cell of the candidate MR ($\mathrm{MR_{Nb2\_RSRP}}$) must be 20 dB lower than the RSRP of its serving cell ($\mathrm{MR_{Serv\_RSRP}}$) is requested on the basis of possessing the same cell ID. When $\mathrm{REQ_{Nb}} \geq 2$, the MR is selected as long as its $\mathrm{Serv_{ID}}$ or $\mathrm{Nb1_{ID}}$ is the same as $\mathrm{Serv_{ID}}$ or $\mathrm{Nb1_{ID}}$ of the REQ. When $\mathrm{REQ_{Nb}} = 0$, if $\mathrm{MR_{Nb}} = 0$, only $\mathrm{MR_{Serv\_ID}} = \mathrm{REQ_{Serv\_ID}}$ is required; otherwise, it is also necessary that the RSRP of the first neighboring cell ($\mathrm{MR_{Nb1\_RSRP}}$) is much less than $\mathrm{MR_{Serv\_RSRP}}$.

The similarity of the candidate MRs subjected to the data filtering mechanism needs to be calculated to select the closest fingerprint. The similarity of the nth fingerprint record is denoted as $d(n)$, and the degree of similarity decreases with the increase in $d(n)$. The LMS-based method is defined as

$$d(n) = \sqrt{\frac{\sum_i (f_i - g_i(n))^2 + \sum_j \left(f_j - l_{\min}\right)^2}{M}} \tag{2}$$

where f_i and $g_i(n)$ denote the RSRP of the REQ and the RSRP of the nth MR in the ith cell, respectively. $l_{\min}$ represents the missing signal level values, which is used to penalize the cells that are not matched in the REQ. M is the total number of sum of summations. Therefore, a larger $d(n)$ results a smaller similarity. The similarity calculation process is as follows (see Fig. 6). We traverse all the cells in the REQ, and it should be noted that the comparison between REQ and alternative MR is based on the cells of REQ. If the cell in the REQ is not in the MR, the penalty from the second summation in the formula is generated. Therefore, when $\mathrm{REQ_{Nb}} \geq 2$, $d(n)$ and the corresponding $l_{\min}$ are set, while there is no need to consider the second summation of the formula when the neighboring cell of REQ is 0 or 1.

2) Similarity Adjustment According to TA: TA can be converted into the distance between REQ and the serving cell, which is set as parameter T_a. As defined in 3GPP [42], $1T_a = 16 \times T_s = 16/(15\,000 H_z \times 2048) \approx 0.52\ \mu$s, where T_s is the elementary time unit of the LTE network, so $1T_a$ map to the distance between eNB and UE is $(300\,000\ \text{km/s} \times 0.52\ \mu\text{s})/2 = 78$ m. The similarity between REQ and MR is estimated and adjusted with the TA Factor. First, find the longitude and latitude of the serving cell of REQ in the cell database, and calculate its distance from the MR. Then, the actual distance from the user to the serving cell is estimated according to the TA of the REQ, and the two distance values are compared. If the distances are consistent within a certain range, the similarity cannot be changed; otherwise, the similarity can be adjusted.

3) WKNN Algorithm: After using the data filtering mechanism to select candidate fingerprints, we calculate the similarity of each fingerprint data according to the similarity calculation rule. Then, the similarity can be used as the weight coefficient in the WKNN algorithm to obtain the predicted position, which is expressed by the latitude and longitude of the center of the generated ellipse.

According to the WKNN algorithm, select K MRs to estimate the final position, and the estimated position (EstPos) can be given by

$$\mathrm{EstPos} = \sum_{n=1}^{K} (w(n) \times P(n)) \tag{3}$$

where $P(n)$ is the position of the nth fingerprint record, and $w(n)$ can be given by

$$w(n) = \frac{\frac{1}{d(n)}}{\sum_{n=1}^{K} \frac{1}{d(n)}} \tag{4}$$

where $d(n)$ is the similarity of each fingerprint record.

IV. Result Analysis

More than 56 000 MRs are captured in the commercial cellular network of typical urban areas by drive test with TEMS. Fig. 7 shows the RSRP distribution of the serving cell and its neighboring cells in the first 600 fingerprint records in the MR. The RSRP is roughly concentrated in the range of -75 to -95 dBm, and the RSRP of the serving cell is higher than that of the neighboring cells, which is suitable for the actual situation.

In the process of scenario sensing, about 56% of the fingerprints are selected for training the random forest model, and the remaining are used as the test set for classification prediction and subsequent positioning. In the process of RF fingerprinting positioning, 75% of the 24 456 fingerprint records are randomly selected to construct a fingerprint database, and the others are used as the positioning test data. Since massive fingerprints of UEs are recorded by MDT, the REQs of the users in different locations and the MRs in the database are overlapped to a large extent. Therefore, 50% of the fingerprints in the test set are randomly selected and put back into the database to ensure the result more realistic.

Positioning precision (error) and positioning accuracy (probability) are selected as evaluation indicators of the positioning system. Positioning precision is the error between the obtained data and the real data. Positioning accuracy judges the correct positioning result. In a word, precision and

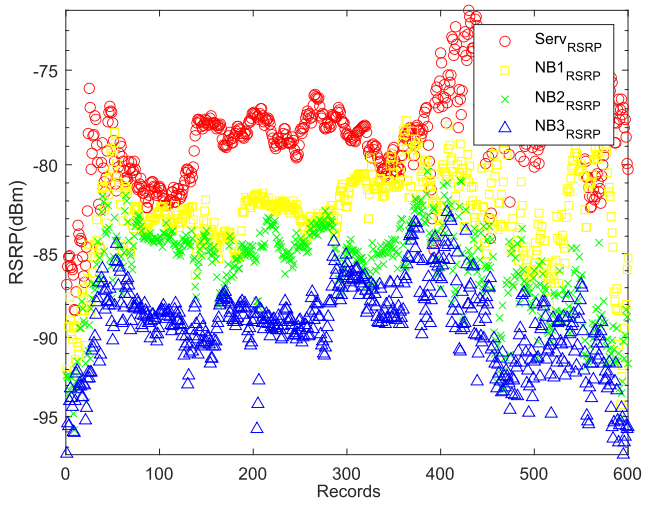

Fig. 7. RSRP distribution of the serving and neighboring cells.

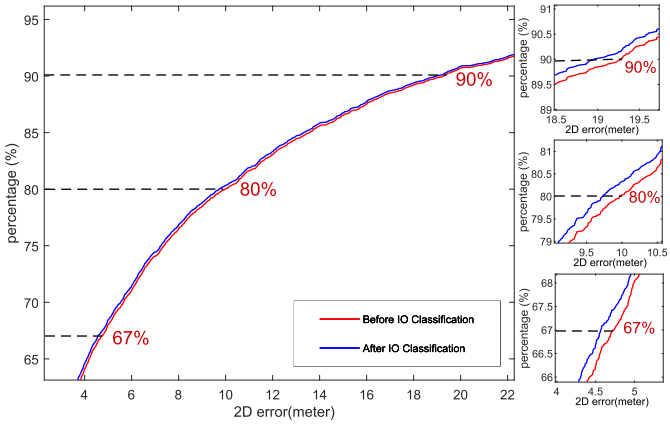

Fig. 8. CDF for comparison of the positioning results.

TABLE IV
COMPARISON OF POSITIONING ERROR UNDER DIFFERENT POSITIONING PROBABILITIES

Fingerprint Database	error(m) 67%	80%	90%
I + O	4.7392	9.9728	19.2860
O	4.5688	9.7305	18.9559
Improvement	4%	2%	2%

accuracy are two contradictory concepts in positioning, which need to be balanced according to practical application. The location of the UE positioning requirements is determined by FCC for a mobile operator, which is within 100 m for 67% and 300 m for 90% [7].

The probability of the positioning error in the range of x is defined by cumulative density function (cdf). The size of the error is shown in the horizontal axis, and the error distribution is shown in the vertical axis. Fig. 8 shows comparison of the cdf of the original positioning results with the results after filtering indoor fingerprints. The probability growth trend is similar to the positioning error, and the probability after denoising is more precise when the positioning error is constant.

Table IV visualizes the positioning error in different positioning probabilities before and after denoising. When the positioning probability reaches 67%, the positioning error is marked as "67% error." The following conclusions are obtained from the table.

TABLE V
COMPARISON OF THE RESULTS FROM DIFFERENT POSITIONING METHODS

Positioning method	error(m) 67%	80%	90%
SVM-based	9.3752	26.0731	85.6246
WKNN-based	9.1351	23.9426	79.4932
Improved WKNN-based/	**4.7392**	**9.9728**	**19.2860**

1) The original positioning result outperformed the FCC positioning requirements, which rises the difficulty of reducing the positioning error as well.
2) Precision and accuracy are two contradictory concepts in positioning, which need to be balanced during the whole data processing procedure.
3) If the probability maintains the same, the overall positioning error can be reduced using the IO classifier to filter the positioning fingerprints or promoting the position precision. In particular, the positioning error after denoising is reduced by about 4% when the probability is 67%, and the positioning error is reduced by 2% when the probability is 80% and 90%. In conclusion, the positioning accuracy improves significantly in case of the probability decreasing.

A. Comparative Experiment

The proposed method is compared with the state-of-the-art (SOA) to better demonstrate its effectiveness. An in-depth analysis of IO classification is conducted in our previous paper [41], and experiments reveal that random forest can efficiently classify indoor and outdoor fingerprints and reduce the data dimensionality. In comparison to other popular ML algorithms such as support vector machine (SVM) or KNN, the ensemble learning method could process the vast data with a large amount of variables, and the capability of dealing with unlabeled data promoted random forest to be an optimal choice for IO classification based on cellular big data. Moreover, SVM and WKNN are also widely used for IO localization [13], and thus, we choose these two methods to compare with the proposed improved WKNN-based localization method. Since the WKNN algorithm is included in the proposed method, the parameter settings are consistent. In addition, the SVM is trained with the radial basis function (RBF) kernel and the regularization parameter $C = 20$. The results in Table V demonstrate that SVM performs slightly worse since it is better suited to sparse and small sample data. Moreover, when compared with WKNN, our proposed method based on the improved WKNN is able to significantly improve the positioning precision. This occurs as a result of the addition of a data filtering mechanism prior to positioning, which effectively lessens the positioning error and calculation.

For further analysis, we take the problem of whether the reduction of data in the fingerprint database caused by denoising has an influence on the positioning system

TABLE VI
POSITIONING ERROR OF DATABASE COMPARATIVE EXPERIMENTS

Database (Data size)		error(m) 67%	error(m) 90%
I + O (21398 × 29)		4.7392	19.2860
O (18022 × 29)		4.5688	18.9559
Database comparative experiments (18022 × 29)	once	5.3537	21.3243
	Cubic average	5.3669	21.3343
	Quintic average	5.4024	21.3278
	Ten times average	5.3862	21.4067

performance into consideration. Comparative experiments of randomly removing fingerprints based on the raw database are performed, and it has to be noted that the same amount of data as the indoor fingerprints are supposed to be randomly removed to ensure the consistency of data size.

Ten comparative experiments are performed based on the raw fingerprint database (I + O). Table VI indicates that no matter how many experiments are performed, the positioning error is larger than that after denoising with the same amount of data when the probability is the same. On one hand, the noise interference of positioning caused by indoor fingerprints need not be removed completely in the process of randomly removing MRs. On the other hand, the reduction of outdoor effective fingerprints also leads to an increase in positioning error. Moreover, the positioning error of comparative experiments is also larger than the raw data, which means the reduction of data is unable to improve the positioning precision, but worsens the positioning performance.

B. Positioning Error Under Different K Values

The initial K value is set to 8 in this article. The positioning results under different K values are analyzed based on the WKNN matching algorithm. K is selected as 1, 2, 4, 6, 8, and 10, respectively, to locate based on the fingerprint database before and after denoising.

The positioning error generally decreases first and then increases with K when the WKNN algorithm is simply used. When K is small, the algorithm is prone to be interfered by abnormal points. Once a point with a large error appears, it is difficult to use other adjacent points to correct the error. When K is larger, there are more nearby points to correct the error so that the error is reduced. However, when K is too large, the positioning error also becomes larger due to the increase in nearby points far away from the UE [43], [44].

The positioning error with 67% and 90% is obtained in Fig. 9. It shows that the positioning error after fingerprint denoising becomes smaller regardless of the value of K, which further proves the effectiveness of removing the noise interference of indoor data for improving positioning precision. However, the positioning errors before and after database denoising increase with K in Fig. 9(a), which is different from the general situation. This is because we have screened the fingerprints twice in the previous steps of the RF fingerprinting positioning, in addition to using the WKNN algorithm for location matching. As a result, the points with

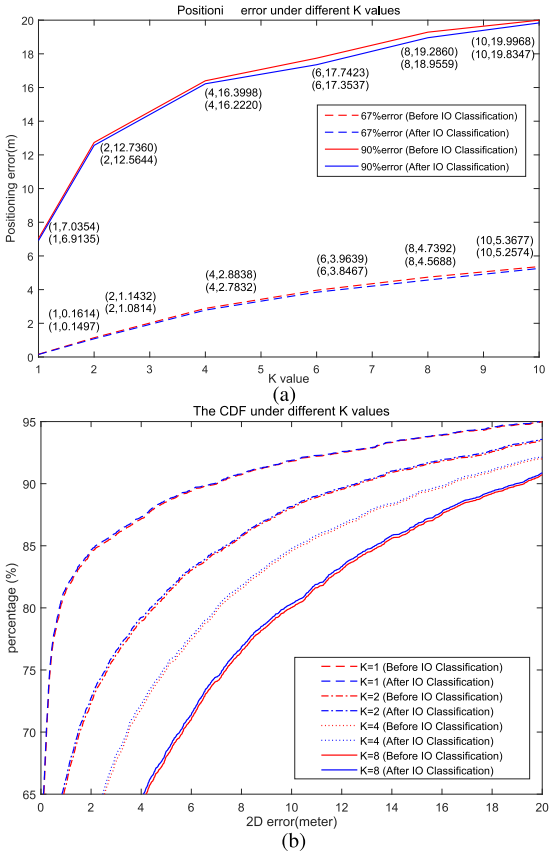

Fig. 9. Positioning results under different K values. (a) Positioning error under different K values. (b) CDF under different K values.

large error have been filtered out. Therefore, REQ can be directly matched to the same or the most similar MRs in the fingerprint database when $K = 1$. And the MRs far away from UE rise with the increase in K, which results in a reduction of positioning performance.

The cdf under different K values is shown in Fig. 9(b), which indicates the positioning performance is best when $K = 1$. It is worth noting that limited MRs are collected in the drive test, while massive MRs are automatically reported by UEs at various scenarios in actual situations. Therefore, the choice of K value cannot be generalized, but needs to be analyzed according to the databases with different data sizes and distributions.

C. Positioning Error Under Different Data Return Ratios

Massive fingerprint records of UEs are automatically uploaded to the server by MDT in the actual situation. About 50% of the fingerprints from the REQs are randomly selected to put back into the database so as to meet the actual situation that there is overlap between REQs and MRs. To explore the impact of data return ratio on positioning error, we randomly select 25%, 50%, and 75% of the REQs to put back into the fingerprint database.

The positioning error of different data return ratios under different K values is shown in Table VII. Regardless of the data return ratio, the positioning error increases with an increase in K and decreases after fingerprint denoising, which

TABLE VII
POSITIONING ERROR UNDER DIFFERENT DATA RETURN RATIOS

Data Return Ratio (Data size)	K value	67%error(m) Before IO	67%error(m) After IO	67%error(m) Improvement	90%error(m) Before IO	90%error(m) After IO	90%error(m) Improvement
25% (I + O: 19870 × 29)	2	2.5561	2.5494	1%	19.6940	19.6701	2%
	4	4.5738	4.5683	0.1%	21.6530	21.5315	0.6%
	6	5.5866	5.5866	0%	22.8524	22.7877	0.3%
	8	6.4323	6.4319	0%	23.8070	23.7434	0.2%
50% (I + O: 21398 × 29)	2	1.1353	1.0779	5%	12.7360	12.5644	1%
	4	2.8813	2.7818	3%	16.3998	16.2220	1%
	6	3.9506	3.8465	3%	17.7423	17.3537	2%
	8	**4.7392**	**4.5688**	**4%**	**19.2860**	**18.9559**	**2%**
75% (I + O: 22927 × 29)	2	0.4593	0.4074	11%	6.6456	6.5112	2%
	4	1.9254	1.7879	7%	10.5385	10.1786	3%
	6	2.8202	2.6680	5%	12.7802	12.4152	3%
	8	3.5307	3.3764	3%	14.6313	14.2391	3%

TABLE VIII
COMPARISON OF POSITIONING ERROR BEFORE AND AFTER IO CLASSIFICATION FOR REQS

REQ (Data size)	Data-base	error(m) 67%	error(m) 80%	error(m) 90%
I + O (6115 × 29)	I + O	4.7392	9.9728	19.2860
	O	4.5688	9.7305	18.9559
O (5140 × 29)	I + O	5.9343	11.4681	21.3452
	O	5.9343	11.4681	21.3452
Comparative experiment I + O (5140 × 29)	I + O	4.9192	10.1364	19.3330
	O	4.7350	9.8559	18.9500

TABLE IX
POSITIONING ERROR UNDER DIFFERENT DATABASES

Database (Data size)	error(m) 67%	error(m) 80%	error(m) 90%
DI + MI + O (21398 × 29)	4.7392	9.9728	19.2860
MI + O (19129 × 29)	**4.4335**	**9.5241**	**18.7785**
O (18022 × 29)	4.5688	9.7305	18.9559
Comparative experiment DI + MI + O(19129 × 29)	5.0766	10.7510	20.7854
Comparative experiment MI + O(18022 × 29)	4.6453	10.2971	19.4229

is consistent with earlier observations. Moreover, with the increase in fingerprint records in the database, the positioning error decreases following the increase in the data return ratio, and there is a more significant error change.

D. IO Classification for REQs

Since the REQs contain both the outdoor data and indoor data, which are unable to be accurately estimated, IO classification for REQs needs to be used to extract outdoor REQs to investigate the effect of database IO classification on outdoor positioning error. [I + O] represents the data before IO classification, and [O] represents the outdoor data obtained after IO classification.

The effect of fingerprint denoising on outdoor positioning error is discussed in Table VIII. For outdoor positioning, the same positioning error is achieved before and after filtering out indoor MRs. It means if the REQ is marked as outdoors, the amount of data is reduced by database preprocessing, and hence the efficiency of positioning and the utilization of the database are improved.

The positioning error is unable to be compared accurately due to the different amount of REQs, so comparative experiment is performed based on the raw REQ[I + O]. As a result, the amount of the remaining REQs which come from both indoors and outdoors is the same as REQ[O]. As shown in Table VIII, the overall positioning error of REQs comparative experiment is smaller than that of REQ[O] with the same data size, which indicates that some indoor REQs are able to be successfully located. Although the GPS carried by some indoor data is biased, it is still used for positioning. It is also located successfully with small error due to the smaller indoor area and the more concentrated sampling.

In addition, the change regularity of the positioning error before and after denoising is the same as that of the raw REQ[I + O]. Moreover, the reduction of the total amount of REQs leads to the reduction of effective positioning REQs, so the positioning error becomes larger.

E. Further Classification for Database

Since part of the indoor fingerprints with biased GPS are able to be used for positioning, indoor MRs are further divided into DI (DI fingerprints without GPS) and MI (MI fingerprints with GPS) by judging whether there is GPS information. The positioning error under different databases is shown in Table IX, where REQs belong to "I + O."

The positioning error of further retaining MI MRs is smaller than that of only outdoor MRs kept. This is because MI fingerprints in the database are used to achieve positioning for some indoor REQs with less error. It should be noted that although these indoor REQs can be successfully located, the EstPos is inaccurate due to the inherent deviation of GPS. Although GPS is unable to be used for indoor positioning, it is collected near windows or in a semi-indoor scenario similar to a balcony (see Fig. 2), which leads to the results that the estimated location is outdoor with its actual location indoor. Therefore, the reliability of the EstPos obtained in this case is low.

Similarly, comparative experiments are conducted to eliminate the impact of different data sizes on positioning error for further classifications. Table IX indicates that the positioning error of comparative experiment of database [DI + MI + O] becomes larger due to the deletion of the effective positioning MRs [MI + O] and the retention of invalid DI fingerprints. Although effective MI fingerprint records are retained in the database, some outdoor MRs are lost at the same time in the comparative experiment of database [MI + O]. In this case, the positioning error varies according to the ratio of MI and outdoor MRs. The outdoor positioning error is larger than the indoor error, so it has a greater effect on the overall error. In brief, the positioning error increases due to the reduction of outdoor MRs.

In addition, the framework of integrated IO sensing and positioning is better realized when REQs are also further classified before positioning. We use communication signals to sense the mobile scenarios where UEs report REQs, and then match REQs with the classified MRs in the database. On one hand, the positioning precision and efficiency are improved. On the other hand, different judgments are made on the results obtained in different scenarios, and then targeted researches are conducted to improve the performance.

V. Conclusion

In this article, we present an ML-based integrated IO sensing and positioning framework for sensing the mobile scenarios and reducing the positioning error based on the MRs obtained in the commercial cellular network. By comparing the positioning error, preprocessing the database using the IO classifier is proven to be effective in filtering fingerprints for RF fingerprinting positioning (the accuracy of IO classification reaches up to 97%). The integrated IO sensing and positioning approach gives smaller positioning error and offers further personalized services based on the refined contextualizations, compared with the conventional fingerprint-based positioning. Moreover, five evaluation experiments are conducted to analyze the results, making the framework more convincing and universal. The proposed framework is suitable for MDT by which users automatically upload massive data, thus can be easily extended to more refined and dynamic scenario sensing and positioning tasks for HCS upgrades.

As for future work, we consider filling in more accurate GPS for indoor MRs to reduce the deviation of indoor positioning. According to the radio propagation rules, the GPS of indoor MR is replaced with that of the most similar outdoor MR. Moreover, the existing outdoor data are able to be used for trajectory prediction to provide better personalized services.

References

[1] T. Wild, V. Braun, and H. Viswanathan, "Joint design of communication and sensing for beyond 5G and 6G systems," *IEEE Access*, vol. 9, pp. 30845–30857, 2021.

[2] D. K. Pin Tan et al., "Integrated sensing and communication in 6G: Motivations, use cases, requirements, challenges and future directions," in *Proc. 1st IEEE Int. Online Symp. Joint Commun. Sens. (JC&S)*, Feb. 2021, pp. 1–6.

[3] N. Khiadani, "Vision, requirements and challenges of sixth generation (6G) networks," in *Proc. 6th Iranian Conf. Signal Process. Intell. Syst. (ICSPIS)*, Dec. 2020, pp. 1–4.

[4] V. P. Rekkas, S. Sotiroudis, P. Sarigiannidis, G. K. Karagiannidis, and S. K. Goudos, "Unsupervised machine learning in 6G networks -state-of-the-art and future trends," in *Proc. 10th Int. Conf. Modern Circuits Syst. Technol. (MOCAST)*, Jul. 2021, pp. 1–4.

[5] Z. Li, K. Xu, H. Wang, Y. Zhao, X. Wang, and M. Shen, "Machine-learning-based positioning: A survey and future directions," *IEEE Netw.*, vol. 33, no. 3, pp. 96–101, May 2019.

[6] *Enhanced 911—Wireless Services*. Accessed: Jul. 25, 2017. [Online]. Available: https://www.fcc.gov/general/enhanced-9-1-1-wireless-services

[7] (Sep. 2011). *Ericsson White Paper, Postioning With LTE*. [Online]. Available: https://www.sharetechnote.com/Docs/WP-LTE-positioning.pdf

[8] (Feb. 2012). *Spirent White Paper: An Overview of LTE Positioning*, [Online]. Available: https://www.spirent.com/media/White

[9] *3GPP Release 9*. Accessed: Jul. 1, 2016. [Online]. Available: http://www.3gpp.org/specifications/releases/71-release-9

[10] R. Margolies et al., "Can you find me now? Evaluation of network-based localization in a 4G LTE network," in *Proc. IEEE Conf. Comput. Commun.*, May 2017, pp. 1–9.

[11] Q. D. Vo and P. De, "A survey of fingerprint-based outdoor localization," *IEEE Commun. Surveys Tuts.*, vol. 18, no. 1, pp. 491–506, 1st Quart., 2015.

[12] H. Sun et al., "Fingerprinting-based outdoor localization with 28-GHz channel measurement: A field study," in *Proc. IEEE 21st Int. Workshop Signal Process. Adv. Wireless Commun. (SPAWC)*, May 2020, pp. 1–5.

[13] L. Polak, S. Rozum, M. Slanina, T. Bravenec, T. Fryza, and A. Pikrakis, "Received signal strength fingerprinting-based indoor location estimation employing machine learning," *Sensors*, vol. 21, no. 13, p. 4605, Jul. 2021.

[14] P.-C. Lin, "Minimization of drive tests using measurement reports from user equipment," in *Proc. IEEE 3rd Global Conf. Consum. Electron. (GCCE)*, Oct. 2014, pp. 84–85.

[15] B. Lee, C. Lim, and K. Lee, "Classification of indoor-outdoor location using combined global positioning system (GPS) and temperature data for personal exposure assessment," *Environ. Health Preventive Med.*, vol. 22, p. 29, Apr. 2017.

[16] R. S. Pissardini and E. S. Fonseca Junior, "Automatic detection of indoor and outdoor scenarios using NMEA message data from GPS receivers," *Revista Brasileira de Geomática*, vol. 6, no. 4, pp. 346–360, 2018.

[17] Y. Zhu et al., "A fast indoor/outdoor transition detection algorithm based on machine learning," *Sensors*, vol. 19, no. 4, p. 786, 2019.

[18] H. Zou, H. Jiang, Y. Luo, J. Zhu, X. Lu, and L. Xie, "BlueDetect: An iBeacon-enabled scheme for accurate and energy-efficient indoor-outdoor detection and seamless location-based service," *Sensors*, vol. 16, no. 2, p. 268, Feb. 2016.

[19] H. Mizuno, K. Sasaki, and H. Hosaka, "Indoor-outdoor positioning and lifelog experiment with mobile phones," in *Proc. Workshop Multimodal Interfaces Semantic Interact. (WMISI)*, 2007, pp. 55–57.

[20] I. Ashraf, S. Hur, and Y. Park, "MagIO: Magnetic field strength based Indoor- outdoor detection with a commercial smartphone," *Micromachines*, vol. 9, no. 10, p. 534, Oct. 2018.

[21] Z. Liu, H. Park, Z. Chen, and H. Cho, "An energy-efficient and robust indoor-outdoor detection method based on cell identity map," *Proc. Comput. Sci.*, vol. 56, pp. 189–195, Jul. 2015.

[22] M. Li, P. Zhou, Y. Zheng, Z. Li, and G. Shen, "IODetector: A generic service for indoor/outdoor detection," *ACM Trans. Sen. Netw.*, vol. 11, no. 1, pp. 1–29, 2015.

[23] S. Li et al., "A lightweight and aggregated system for indoor/outdoor detection using smart devices," *Future Gener. Comput. Syst.*, vol. 107, pp. 988–997, Jun. 2020.

[24] W. Wang, Q. Chang, Q. Li, Z. Shi, and W. Chen, "Indoor-outdoor detection using a smart phone sensor," *Sensors*, vol. 16, no. 10, p. 1563, Sep. 2016.

[25] I. Rodriguez, H. C. Nguyen, I. Z. Kovács, T. B. Sørensen, and P. Mogensen, "An empirical outdoor-to-indoor path loss model from below 6 GHz to cm-wave frequency bands," *IEEE Antennas Wireless Propag. Lett.*, vol. 16, pp. 1329–1332, 2016.

[26] A. Kaya and D. Calin, "On the wireless channel characteristics of outdoor-to-indoor LTE small cells," *IEEE Trans. Wireless Commun.*, vol. 15, no. 8, pp. 5453–5466, Aug. 2016.

[27] S. Fischer, "Observed time difference of arrival (OTDOA) positioning in 3GPP LTE," Qualcomm Technol., San Diego, CA, USA, Jun. 2014. [Online]. Available: https://www.mendeley.com/catalogue/5223904d-746e-3774-961b-768cc5cdb507/ and https://www.qualcomm.com/content/dam/qcomm-martech/dm-assets/documents/otdoa_positioning_in_3gpp_lte_v1.pdf

[28] *Study on NR Positioning Support*, 3GPP document TR 38.855, vol. 16, Mar. 2019.
[29] S. Zhang, J. Li, and S. Chen, "5G NR positioning technology and its deployment scheme," *ZTE Technol. J.*, vol. 27, no. 2, pp. 49–53, 2016.
[30] *Radio Frequency (RF) Pattern Matching Location Method in LTE*, 3GPP document TR 36.809, vol. 12, Sep. 2013.
[31] H. Aly and M. Youssef, "Dejavu: An accurate energy-efficient outdoor localization system," in *Proc. 21st ACM SIGSPATIAL Int. Conf. Adv. Geographic Inf. Syst. (ACM-GIS)*, vol. 27, 2013, pp. 154–163.
[32] X. Tian, X. Wu, H. Li, and X. Wang, "RF fingerprints prediction for cellular network positioning: A subspace identification approach," *IEEE Trans. Mobile Comput.*, vol. 19, no. 2, pp. 450–465, Feb. 2020.
[33] A. Viel et al., "Map matching with sparse cellular fingerprint observations," in *Proc. Ubiquitous Positioning, Indoor Navigat. Location-Based Services (UPINLBS)*, Mar. 2018, pp. 1–10.
[34] N. A. Maung Maung, B. Y. Lwi, and S. Thida, "An enhanced RSS fingerprinting-based wireless indoor positioning using random forest classifier," in *Proc. Int. Conf. Adv. Inf. Technol. (ICAIT)*, Nov. 2020, pp. 59–63.
[35] J.-Y. Lee, C. Eom, Y. Kwak, H.-G. Kang, and C. Lee, "Dnn-based wireless positioning in an outdoor environment," in *Proc. IEEE Int. Conf. Acoust., Speech Signal Process. (ICASSP)*, Apr. 2018, pp. 3799–3803.
[36] C. Zhang, P. Patras, and H. Haddadi, "Deep learning in mobile and wireless networking: A survey," *IEEE Commun. Surveys Tuts.*, vol. 21, no. 3, pp. 2224–2287, 3rd Quart., 2019.
[37] M. M. Butt, A. Rao, and D. Yoon, "RF fingerprinting and deep learning assisted UE positioning in 5G," in *Proc. IEEE 91st Veh. Technol. Conf. (VTC-Spring)*, May 2020, pp. 1–7.
[38] K. N. R. S. V. Prasad, E. Hossain, and V. K. Bhargava, "Machine learning methods for RSS-based user positioning in distributed massive MIMO," *IEEE Trans. Wireless Commun.*, vol. 17, no. 12, pp. 8402–8417, Dec. 2018.
[39] S.-I. Sou, W.-H. Lin, K.-C. Lan, and C.-S. Lin, "Indoor location learning over wireless fingerprinting system with particle Markov chain model," *IEEE Access*, vol. 7, pp. 8713–8725, 2019.
[40] *TEMS*. Accessed: Aug. 2, 2021. [Online]. Available: https://www.infovista.com/tems
[41] L. Zhang, Q. Ni, M. Zhai, J. Moreno, and C. Briso, "An ensemble learning scheme for indoor-outdoor classification based on KPIs of LTE network," *IEEE Access*, vol. 7, pp. 63057–63065, 2019.
[42] *Physical Layer Procedures (Release 8)*, document 3GPP TS 36.213 V8.6.0, Mar. 2009.
[43] B. Wang, Y. Zhao, T. Zhang, and X. Hei, "An improved integrated fingerprint location algorithm based on WKNN," in *Proc. 29th Chin. Control Decis. Conf. (CCDC)*, May 2017, pp. 4580–4584.
[44] A. Gholoobi and S. Stavrou, "RSS based localization using a new WKNN approach," in *Proc. 7th Int. Conf. Comput. Intell., Commun. Syst. Netw.*, Jun. 2015, pp. 27–30.

Lei Zhang (Member, IEEE) received the B.S. degree in communication engineering from Anhui University, Hefei, China, in 2009, and the M.S. and Ph.D. degrees in telecommunications from the Universidad Politécnica de Madrid (UPM), Madrid, Spain, in 2013 and 2016, respectively.

In 2016, he was a Visiting Scholar with the University of South Carolina, Columbia, SC, USA. From 2016 to 2017, he was a Research Assistant Professor with the Shanghai Institute of Microsystem and Information Technology, Chinese Academy of Sciences, Shanghai, China. Since 2019, he has been an Associate Professor with the College of Information Science and Technology, Donghua University, Shanghai. His research interests include wireless channel sounding and modeling, and wearable computing.

Dr. Zhang has received the Premio Extraordinario de Doctorado (Extraordinary Ph.D. Award).

Xin Chu is currently pursuing the master's degree in information and communication engineering with the College of Information Science and Technology, Donghua University, Shanghai, China.

Her research interests include cellular network localization and trajectory prediction.

Menglin Zhai (Member, IEEE) received the B.S. degree in information science and engineering from Southeast University, Nanjing, China, in 2010, and the Ph.D. degree in electromagnetic fields and microwave techniques from Shanghai Jiao Tong University, Shanghai, China, in 2016.

Since August 2016, she has been an Associate Professor with the College of Information Science and Technology, Donghua University, Shanghai. Her current research interests include computational electromagnetics and applications especially the finite-difference time-domain (FDTD) method, electro magnetic interference (EMI)/electro magnetic compatibility (EMC) analysis, wireless communication simulation, and nanotechnology.